

# ChemComm

Accepted Manuscript



This article can be cited before page numbers have been issued, to do this please use: J. Wu, Y. Li, C. Tan, X. Wang, Y. Zhang, J. Song, J. Qu and W. (. Wong, *Chem. Commun.*, 2018, DOI: 10.1039/C8CC06839A.



This is an Accepted Manuscript, which has been through the Royal Society of Chemistry peer review process and has been accepted for publication.

Accepted Manuscripts are published online shortly after acceptance, before technical editing, formatting and proof reading. Using this free service, authors can make their results available to the community, in citable form, before we publish the edited article. We will replace this Accepted Manuscript with the edited and formatted Advance Article as soon as it is available.

You can find more information about Accepted Manuscripts in the [author guidelines](#).

Please note that technical editing may introduce minor changes to the text and/or graphics, which may alter content. The journal's standard [Terms & Conditions](#) and the ethical guidelines, outlined in our [author and reviewer resource centre](#), still apply. In no event shall the Royal Society of Chemistry be held responsible for any errors or omissions in this Accepted Manuscript or any consequences arising from the use of any information it contains.



Journal Name

COMMUNICATION

## Aggregation-induced near-infrared emitting platinum(II) terpyridyl complex: cellular characterisation and lysosome-specific localisation†

Received 00th January 20xx,  
Accepted 00th January 20xx

DOI: 10.1039/x0xx00000x

www.rsc.org/

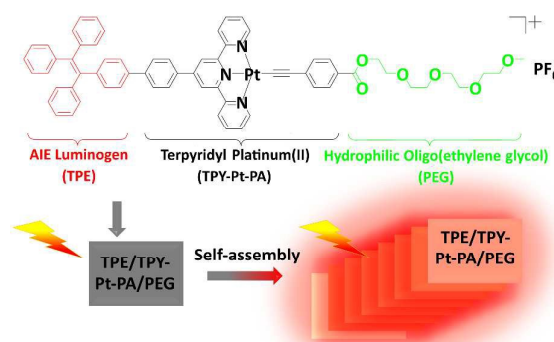
Jiatao Wu,<sup>a,b</sup> Yaqiong Li<sup>c</sup>, Chunyan Tan,<sup>d,e</sup> Xin Wang,<sup>a</sup> Youming Zhang,<sup>a,b</sup> Jun Song,<sup>\*a</sup> Junle Qu,<sup>\*a</sup> and Wai-Yeung Wong<sup>\*a,b</sup>

A novel near-infrared luminogen (TPE/TPY-Pt-PA/PEG) based on the terpyridyl Pt(II) complex with a tetraphenylethene periphery is synthesised and characterised. It displays aggregation-induced emission with the formation of self-assembled nanostructures. The nanoparticles fabricated with TPE/TPY-Pt-PA/PEG show excellent biocompatibility with high specificity to lysosomes in HeLa cells.

Near-infrared (NIR) fluorophores have received a great deal of attention during the past decades because of their extensive applications in organic light-emitting diodes,<sup>1</sup> therapy<sup>2</sup> and bioimaging.<sup>3,4</sup> Although the most widely used commercial NIR fluorescent probes are organic fluorophores,<sup>5</sup> transition-metal complexes have highly promising prospects in imaging<sup>6</sup> because of several important advantages, including outstanding photostability, long excited-state lifetimes, large Stokes shift and high emission quantum yields.<sup>7</sup>

Among the various transition-metal complexes applied in cellular imaging,<sup>8-10</sup> Pt(II) complexes show ligand to ligand charge transfer (LLCT), metal-to-ligand charge transfer (MLCT) and metal-to-metal-ligand charge transfer (MMLCT), which can emit strong emission from the visible to the NIR region. Because of their square-planar geometry, Pt(II) complexes possess attractive biosensing properties, which are due to their high stacking tendency to form high-order supramolecular assemblies.<sup>11-14</sup> To date, several NIR Pt(II) complexes that have been developed hold great promise for *in vivo* imaging.<sup>6</sup> However, low water solubility, aggregation-induced quenching and high phototoxicity still reduce their

possible applications for



Scheme 1 Schematic illustration of AIE active TPE/TPY-Pt-PA/PEG.

imaging.<sup>15, 16</sup> Recently, fluorescent probes with aggregation-induced emission (AIE) characteristics have emerged as an extraordinary class of luminogens for biosensing.<sup>17</sup> AIE materials are weakly emissive or non-emissive in dilute solutions and become highly emissive in an aggregated state. Nevertheless, AIE NIR luminogens based on terpyridyl Pt(II) complexes for bioimaging applications have been rarely reported.

In view of the excellent nature of these two functionalities and their high preference for self-assembly, we have combined the AIE-active tetraphenylethene (TPE)<sup>18</sup> with the terpyridyl Pt(II) complex to fabricate an AIE fluorophore (TPE/TPY-Pt-PA/PEG), leading to bathochromic shifts of both excitation and emission towards more biologically interesting NIR windows. The AIE luminogen is composed of a terpyridyl Pt(II) core which displays strong intermolecular interactions and emissive MMLCT excited states in the aggregate state, a TPE unit which can not only extend  $\pi$ -conjugation of the cyclometalated ligand, but also weaken the strong  $\pi$ - $\pi$  stacking interactions, and a hydrophilic pentaethylene glycol unit that ensure its biocompatibility (Scheme 1). The synthetic route for TPE/TPY-Pt-PA/PEG is shown in Scheme S1 (ESI†). In acetonitrile, TPE/TPY-Pt-PA/PEG is non-emissive, but addition of water

<sup>a</sup> Key Laboratory of Optoelectronic Devices and Systems of Ministry of Education and Guangdong Province, College of Optoelectronic Engineering, Shenzhen University, Shenzhen 518060, P. R. China

<sup>b</sup> Department of Applied Biology and Chemical Technology, The Hong Kong Polytechnic University, Hung Hom, Hong Kong, P. R. China

<sup>c</sup> Shijiazhuang People's Medical College, Shijiazhuang 050091, P. R. China.

<sup>d</sup> Department of Chemistry, Tsinghua University, Beijing 100084, P. R. China

<sup>e</sup> The Ministry-Province Jointly Constructed Base for State Key Lab-Shenzhen Key Laboratory of Chemical Biology, the Graduate School at Shenzhen, Tsinghua University, Shenzhen 518055, P. R. China

† Electronic Supplementary Information (ESI) available: [Detailed experimental methods and additional data.]. See DOI: 10.1039/x0xx00000x

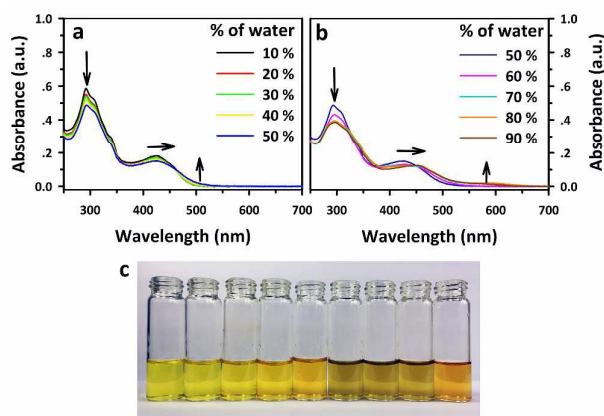


Fig. 1. UV-vis absorption spectra of TPE/TPY-Pt-PA/PEG in acetonitrile (40  $\mu\text{M}$ ) with increasing water content (a) from 10% to 50% and (b) from 50% to 90% (c) Photo showing the colour changes of TPE/TPY-Pt-PA/PEG in acetonitrile at different water proportions (left to right: 10%, 20%, 30%, 40%, 50%, 60%, 70%, 80% and 90% water content).

enhances significantly its NIR emission centred at 730 nm; this can be attributed to the MMLCT emission by the aggregated molecules, along with the restriction of intramolecular rotation of the TPE phenyl rings which facilitate radiative decay channels. The nanoparticles (NPs) fabricated by encapsulating TPE/TPY-Pt-PA/PEG with Pluronic F127 (F127), a commonly used amphiphilic triblock copolymer for drug delivery, lead to the switch-off of toxicity caused by the isolation of platinum(II) complexes and difficult accessibility of the metal center. TPE/TPY-Pt-PA/PEG@F127 NPs exhibit excellent biocompatibility with good performance in lysosome-specific localisation, which demonstrates an excellent molecular modification strategy for Pt(II) complexes for cell imaging.

The optical properties of TPE/TPY-Pt-PA/PEG have been investigated by UV-vis absorption in different solvents (Fig. S4). The photophysical data are summarized in Table S1. There are two main absorption bands: one located at 263–330 nm corresponding to intraligand  $[\pi \rightarrow \pi^*]$  transitions of the alkynyl and terpyridine ligands, and the other located at 375–490 nm attributed to a mixture of  $[d\pi(\text{Pt}) \rightarrow \pi(\text{terpyridine})]$  and  $[\pi(\text{alkynyl}) \rightarrow \pi^*(\text{terpyridine})]$  transitions.<sup>19–21</sup> TPE/TPY-Pt-PA/PEG is non-emissive in good solvents, probably as a result of the fast rotation of the phenyl rings on the TPE moiety. Nevertheless, TPE/TPY-Pt-PA/PEG dissolved in water or ethyl acetate exhibited novel broad absorption bands at around 520–650 nm, which may be induced by molecular aggregates. In addition, the concentration-dependent UV-vis absorption spectra of TPE/TPY-Pt-PA/PEG in acetonitrile (Figures S5) reveal a deviation from Beer's Law at 480 nm which can be assigned to MMLCT transitions, demonstrating that TPE/TPY-Pt-PA/PEG would self-assemble into superstructures in a poor solvent.

Since TPE/TPY-Pt-PA/PEG tends to form molecular aggregates in water (Fig. S4), the UV-vis absorption spectra and dynamic light scattering (DLS) were used in the self-assembly studies of TPE/TPY-Pt-PA/PEG in acetonitrile mixture (40  $\mu\text{M}$ ) with increasing water content. Though the nanoaggregates of TPE/TPY-Pt-PA/PEG become apparent at 20%

water content (Fig. S6a), TPE/TPY-Pt-PA/PEG exhibits a slight bathochromic shift

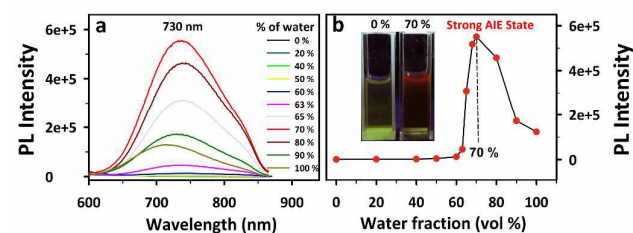


Fig. 2. (a) Photoluminescence (PL) spectra of TPE/TPY-Pt-PA/PEG in acetonitrile/water mixture with different water percentages. (b) Plot of PL intensities of TPE/TPY-Pt-PA/PEG in acetonitrile/water mixture at 730 nm versus water content. Inset: images of TPE/TPY-Pt-PA/PEG in acetonitrile (0% water) and TPE/TPY-Pt-PA/PEG in acetonitrile (70% water), with emission taken under a UV lamp with 355 nm excitation. Conditions:  $[\text{TPE/TPY-Pt-PA/PEG}] = 10 \mu\text{M}$ , excitation wavelength ( $\lambda_{\text{exc}}$ ) = 465 nm.

at the MLCT/LLCT absorption band with an emergence of a low-lying energy absorption tail at about 480–525 nm (Fig. 1a). TPE/TPY-Pt-PA/PEG gives the largest hydrodynamic diameter at 60% water content and the size of the nanoaggregates shows a clear decline with further increasing water content (Fig. S6a). This phenomenon is resulted from the tendency to form more compact nanostructures for minimizing contact of the hydrophobic groups with water. However, the levelling-off absorption tail is still increasing with the weakening of the MLCT/LLCT band (Fig. 1b), suggesting that the weak absorption tail can be assigned as MMLCT absorption due to the formation of molecular aggregates via Pt–Pt interactions,  $\pi$ – $\pi$  interactions or both.

The aggregation induced photoluminescence of TPE/TPY-Pt-PA/PEG in acetonitrile with different water percentages is characterised in Fig. 2. Although the weak absorption tail at 480–525 nm emerges at 20% water content, TPE/TPY-Pt-PA/PEG remains non-emissive. Upon a further increase of the water percentage, a NIR emission band centred at 730 nm is observed and reaches a maximum intensity at a water percentage of 70%. On the basis of the previous spectroscopic studies,<sup>22–24</sup> this emission band can be attributed to the MMLCT emission with enhanced Pt–Pt and/or  $\pi$ – $\pi$  stacking interactions facilitated by the solvent-induced aggregation. Moreover, the aggregation-induced near-infrared emission is also contributed by the restriction of intermolecular rotation of the TPE moiety, which would slow down the non-radiative pathway and facilitate the radiative process. However, the PL intensity of TPE/TPY-Pt-PA/PEG shows a clear decline trend with further increasing water content. A possible reason for this phenomenon is the formation of high-quality nanocrystal particles at 70% water percentage with a low polydispersity index (PDI) of 0.05 (Figure S6b), suggesting that the nanoparticles possess the characteristic of high homogeneity. When the water content exceeds 70%, the TPE/TPY-Pt-PA/PEG gradually aggregates from homogeneous crystal particles to amorphous particles with PDI changing from 0.05 to 0.31, resulting in the reduction of PL intensity.<sup>25, 26</sup> Moreover, TPE/TPY-Pt-PA/PEG would form more compact nanostructures

at high water content, and only the molecules on the surface of the nanoaggregates emitted light upon excitation, which is also an important reason for the decrease of PL intensity.<sup>27</sup>

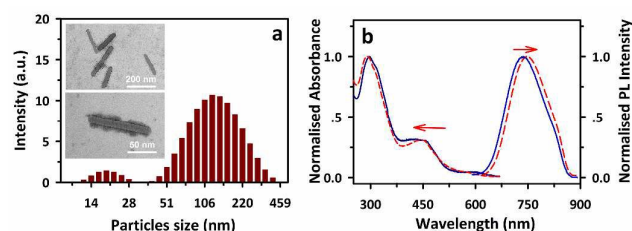


Fig. 3. (a) Particle size distribution of TPE/TPY-Pt-PA/PEG@F127 NPs measured by DLS. Inset: TEM images of AIE NPs with different scale bars. (b) Normalised UV-vis absorption and PL spectra of TPE/TPY-Pt-PA/PEG@F127 NPs (red) and TPE/TPY-Pt-PA/PEG nanoaggregates (blue) in water. [TPE/TPY-Pt-PA/PEG nanoaggregates] = 20  $\mu\text{M}$ ; [TPE/TPY-Pt-PA/PEG@F127 NPs] = 10  $\mu\text{M}$ ;  $\lambda_{\text{ex}}$  = 465 nm.

The aggregation-induced NIR emission of TPE/TPY-Pt-PA/PEG inspires us to explore its cell imaging applications. Since TPE/TPY-Pt-PA/PEG gradually formed unstable aggregates in aqueous media, TPE/TPY-Pt-PA/PEG nanoparticles (abbreviated as TPE/TPY-Pt-PA/PEG@F127 NPs) were fabricated with biocompatible F127 to enhance the stability.<sup>28,29</sup> As shown in

Fig. 3a, the average hydrodynamic diameters for the NPs are 116 nm as measured by DLS; the PDI is 0.31. The percentage of Gaussian-shape distribution intensity at ca. 20 nm and ca. 110 nm is 7.1% and 92.9% respectively, which suggests that TPE/TPY-Pt-PA/PEG@F127 nanoparticles are mainly distributed with the effective diameter at about 110 nm. This was further confirmed by the rod-like shape of the NPs in transmission electron microscopy (Fig. 3a). TPE/TPY-Pt-PA/PEG@F127 NPs were chemically stable for several weeks at room temperature, demonstrating that they were well dispersed in aqueous solution and did not form precipitates.

The photophysical properties of TPE/TPY-Pt-PA/PEG in different states are reported in Table S2. The quantum yield in aqueous solution is greater for TPE/TPY-Pt-PA/PEG nanoaggregates as compared with the solid-state thin film and TPE/TPY-Pt-PA/PEG@F127 NPs. This can be ascribed to the high-quality nanocrystal stacking structure at 70% water percentage. The TPE/TPY-Pt-PA/PEG nanoaggregates showed two absorption maxima at 290 and 445 nm, while the UV-vis absorption spectra of AIE NPs showed slightly red-shifted absorption peaks at 293 and 446 nm (Fig. 3b). The peak emission wavelengths were 730 and 736 nm for TPE/TPY-Pt-PA/PEG nanoaggregates and TPE/TPY-Pt-PA/PEG@F127 NPs, respectively. The excitation and emission profiles of TPE/TPY-Pt-PA/PEG@F127 NPs match well the commercial laser sources and fluorescence-imaging systems, making it promising for bioimaging applications.<sup>30</sup>

A critical consideration for achieving long-term cell tracking is an understanding of the cytotoxicity of NPs. The MTT assay, a colourimetric assay for assessing cell metabolic activity, was used to evaluate the cytotoxicity of TPE/TPY-Pt-PA/PEG@F127 NPs to HeLa cells in the concentration range of 0–100  $\mu\text{M}$  (Fig. S7). Cell viability rates were above 96% at the working

concentration of 20  $\mu\text{M}$ . Even at 100  $\mu\text{M}$ , the cell viability was around 86%, indicating that TPE/TPY-Pt-PA/PEG@F127 NPs have excellent biocompatibility. The NPs for *in vitro* cellular imaging were studied with an Olympus model IX71 inverted microscope. LysoTracker Green was chosen as a commercial

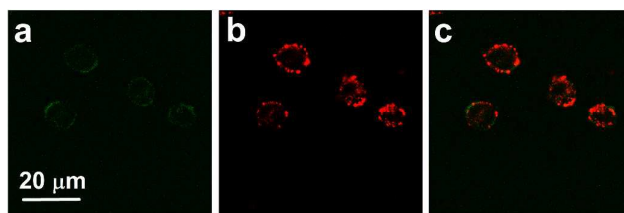


Fig. 4. Confocal laser scanning microscope images of HeLa cervical cancer cells incubated with (a) 100 nM LysoTracker Green ( $\lambda_{\text{ex}}$  = 488 nm, 500–580 nm emission filter) for 30 min and (b) 20  $\mu\text{M}$  TPE-PEG-F127 NPs ( $\lambda_{\text{ex}}$  = 465 nm, 600–750 nm emission filter) for 4 h. (c) The merged images of (a) and (b).

reference to compare the cellular localisation and bioimaging efficiency (Fig. 4a). Intracellular NIR emissions observed upon excitation at 488 nm confirm that these TPE/TPY-Pt-PA/PEG@F127 NPs can be internalised by living cells (Fig. 4b). The intensity profiles across HeLa cells stained with TPE/TPY-Pt-PA/PEG@F127 NPs and LysoTracker Green displayed 88.3% overlap coefficient (Fig. 4c, calculated using Olympus Fluoview ver. 4.2a viewer), indicating that the NPs can preferentially localise in the lysosomes of HeLa cells. The lysosome-specific localisation properties may be derived from the acid–base properties of these terpyridyl complexes.<sup>31</sup> Upon internalisation by endocytosis, TPE/TPY-Pt-PA/PEG@F127 NPs are transported from endosomes to lysosomes, where a significant portion of these complexes become protonated and develop a net positive charge, which causes them to be trapped inside the lysosomes.

In summary, we have combined the AIE-active TPE with the terpyridyl Pt(II) complex to convert the platinum(II) terpyridyl complex into an AIE-active fluorophore (TPE/TPY-Pt-PA/PEG) with bathochromic shifts of both excitation and emission towards more biologically interesting spectral windows. TPE/TPY-Pt-PA/PEG have shown AIE NIR emission and TPE/TPY-Pt-PA/PEG@F127 NPs were found to selectively stain lysosomes in cancer cells with excellent biocompatibility, making them promising candidates for long-term cell tracking. Further studies using the AIE NPs will shed light on the involvement of lysosomes in animal models of lysosomal storage diseases.

Parts of this work were supported by the National Basic Research Program of China (2015CB352005); the National Natural Science Foundation of China (61775145, 31771584, 61605124, 61620106016, 61525503, 61378091, 61405123, 61705143); the Guangdong Natural Science Foundation Innovation Team (2014A030312008); Hong Kong, Macao, and Taiwan cooperation innovation platform & major projects of international cooperation in Colleges and Universities in Guangdong Province (2015KGJHZ002); China Postdoctoral Science Foundation Funded Project (2017M622748, 2018M630979); Shenzhen Basic Research Project

## COMMUNICATION

## Journal Name

(JCYJ20170412110212234, JCYJ20170412105003520, JCYJ20160328144746940, JCYJ20160308093035903, JCYJ20150324141711561, JCYJ20150930104948169). W.-Y.W. thanks Hong Kong Research Grants Council (C6009-17G), Hong Kong Polytechnic University (1-ZE1C) and Ms Clarea Au (847S) for the financial support.

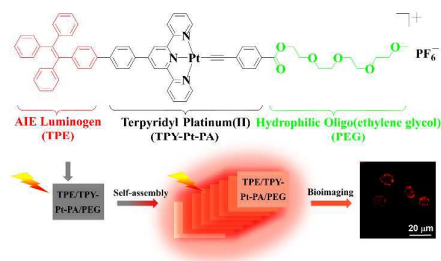
## Conflicts of interest

There are no conflicts to declare

## Notes and references

- C. L. Ho, H. Li and W. Y. Wong, *J. Organomet. Chem.*, 2014, **751**, 261-285.
- S. L. Luo, E. L. Zhang, Y. P. Su, T. M. Cheng and C. M. Shi, *Biomaterials*, 2011, **32**, 7127-7138.
- G. S. Hong, A. L. Antaris and H. J. Dai, *Nat. Biomed. Eng.*, 2017, **1**, 1-22.
- H. G. Lu, Y. D. Zheng, X. W. Zhao, L. J. Wang, S. Q. Ma, X. Q. Han, B. Xu, W. J. Tian and H. Gao, *Angew. Chem., Int. Ed.*, 2016, **55**, 155-159.
- Q. Zheng, M. F. Juetta, S. Jockusch, M. R. Wasserman, Z. Zhou, R. B. Altman and S. C. Blanchard, *Chem. Soc. Rev.*, 2014, **43**, 1044-1056.
- H. F. Xiang, J. H. Cheng, X. F. Ma, X. G. Zhou and J. J. Chruma, *Chem. Soc. Rev.*, 2013, **42**, 6128-6185.
- M. Mauro, A. Aliprandi, D. Septiadi, N. S. Kehr and L. De Cola, *Chem. Soc. Rev.*, 2014, **43**, 4144-4166.
- Y. Chi and P. T. Chou, *Chem. Soc. Rev.*, 2010, **39**, 638-655.
- Q. Zhao, C. Huang and F. Li, *Chem. Soc. Rev.*, 2011, **40**, 2508-2524.
- Q. Zhao, F. Li and C. Huang, *Chem. Soc. Rev.*, 2010, **39**, 3007-3030.
- C. Y.-S. Chung and V. W.-W. Yam, *J. Am. Chem. Soc.*, 2011, **133**, 18775-18784.
- C. Y.-S. Chung, S. P.-Y. Li, K. K.-W. Lo and V. W.-W. Yam, *Inorg. Chem.*, 2016, **55**, 4650-4663.
- M. C.-L. Yeung and V. W.-W. Yam, *Chem. Sci.*, 2013, **4**, 2928-2935.
- C. Y.-S. Chung, S. P.-Y. Li, M.-W. Louie, K. K.-W. Lo and V. W.-W. Yam, *Chem. Sci.*, 2013, **4**, 2453-2462.
- D. L. Ma, H. Z. He, K. H. Leung, D. S. H. Chan and C. H. Leung, *Angew. Chem., Int. Ed.*, 2013, **52**, 7666-7682.
- V. Fernandez-Moreira, F. L. Thorp-Greenwood and M. P. Coogan, *Chem. Commun.*, 2010, **46**, 186-202.
- D. Ding, K. Li, B. Liu and B. Z. Tang, *Acc. Chem. Res.*, 2013, **46**, 2441-2453.
- J. Mei, N. L. Leung, R. T. Kwok, J. W. Lam and B. Z. Tang, *Chem. Rev.*, 2015, **115**, 11718-11940.
- V. W.-W. Yam, K. M.-C. Wong and N. Zhu, *J. Am. Chem. Soc.*, 2002, **124**, 6506-6507.
- A. Aliprandi, M. Mauro and L. De Cola, *Nat. Chem.*, 2016, **8**, 10-15.
- F. C.-M. Leung, S. Y.-L. Leung, C. Y.-S. Chung and V. W.-W. Yam, *J. Am. Chem. Soc.*, 2016, **138**, 2989-2992.
- H. K. Cheng, M. C. L. Yeung and V. W. W. Yam, *ACS Appl. Mater. Interfaces*, 2017, **9**, 36220-36228.
- Z. Zhou, X. Yan, M. L. Saha, M. Zhang, M. Wang, X. Li and P. J. Stang, *J. Am. Chem. Soc.*, 2016, **138**, 13131-13134.
- Y. Sun, K. Ye, H. Zhang, J. Zhang, L. Zhao, B. Li, G. Yang, B. Yang, Y. Wang, S.-W. Lai and C.-M. Che, *Angew. Chem., Int. Ed.*, 2006, **45**, 5610-5613.
- H. Li, Z. Chi, B. Xu, X. Zhang, Z. Yang, X. Li, S. Liu, Y. Zhang and J. Xu, *J. Mater. Chem.*, 2010, **20**, 6103-6110.
- X. Zhang, Z. Chi, B. Xu, C. Chen, X. Zhou, Y. Zhang, S. Liu and J. Xu, *J. Mater. Chem.*, 2012, **22**, 18505-18513.
- R. Liu, S. Zhu, J. Lu, H. Shi and H. Zhu, *Dyes Pigm.*, 2017, **147**, 291-299.
- S. Chen, H. Wang, Y. Hong and B. Z. Tang, *Mater. Horiz.*, 2016, **3**, 283-293.
- W. Qin, K. Li, G. Feng, M. Li, Z. Yang, B. Liu and B. Z. Tang, *Adv. Funct. Mater.*, 2014, **24**, 635-643.
- M. Gao, F. Yu, C. Lv, J. Choo and L. Chen, *Chem. Soc. Rev.*, 2017, **46**, 2237-2271.
- Y.-M. Ho, N.-P. B. Au, K.-L. Wong, C. T.-L. Chan, W.-M. Kwok, G.-L. Law, K.-K. Tang, W.-Y. Wong, C.-H. E. Ma and M. H.-W. Lam, *Chem. Commun.*, 2014, **50**, 4161-4163.

## A table of contents entry



An aggregation-induced near-infrared emitting terpyridyl Pt(II) complex with excellent biocompatibility shows high specificity to lysosomes in HeLa cells.